Vol. 49: 57–69, 2022
https://doi.org/10.3354/esr01202

ENDANGERED SPECIES RESEARCH
Endang Species Res

Published September 29

# Effectiveness of surface-based detection methods for vessel strike mitigation of North Atlantic right whales

**Loïcka M. R. Baille**[1,*], **Daniel P. Zitterbart**[2]

[1]MIT-WHOI Joint Program in Oceanography/Applied Ocean Science & Engineering, 266 Woods Hole Rd, Woods Hole, MA 02543, MA, USA

[2]Applied Ocean Physics and Engineering, Woods Hole Oceanographic Institution, Woods Hole, MA 02543, USA

ABSTRACT: Increasing commercial and recreational use of the world's oceans has led to growing concerns about vessel and marine mammal encounters. For endangered species such as the North Atlantic right whale *Eubalaena glacialis*, reducing the number of vessel strikes is key to improving their protection. In this study, we developed an agent-based model to assess the efficacy of thermal imaging systems as a surface-based whale detection method for vessel strike mitigation. We found that the detection range of such systems is the determining factor for their efficacy and needs to be chosen according to vessel characteristics, such as speed and maneuverability. Furthermore, we found that combining large-scale (e.g. protected zones) and small-scale (e.g. on-board detection systems) mitigation strategies increases protection. Finally, technological improvements are needed to achieve reliable detection ranges beyond what is currently possible so that fast and poorly maneuverable vessels such as ultra-large container ships could benefit from on-board detection systems.

KEY WORDS: *Eubalaena glacialis* · Conservation · Marine mammals · Ship strike · Ship–whale collision · Marine spatial planning · Cetacean

## 1. INTRODUCTION

Increasing anthropogenic marine activities threaten the marine environment. Cetaceans face a multitude of anthropogenic threats, such as vessel strikes, ocean pollution, ocean noise, climate change, fishing gear entanglement, and even whaling in some parts of the world (Sèbe et al. 2019). Vessel strikes and entanglement have become main concerns as the world's oceans have been experiencing an increasing level of use due to growing commercial and recreational activities (Sèbe et al. 2019). In 2020, over 98 000 commercial vessels (>100 gross tons) were documented, a 783 % increase since 1890 (Laist et al. 2001, UNCTAD 2020). This surge in maritime traffic has led to growing concerns that vessel strikes impact marine life welfare and crew safety, and lead to negative economic consequences (Schoeman et al. 2020). With rising interest in autonomous vessels, vessel traffic will continue to grow, further increasing the risk of vessel strikes.

A vessel or ship strike is defined as any physical impact, fatal or not, between any part of a watercraft and a live marine animal (Peel et al. 2018). Vessel strikes are highly concerning, as they affect numerous marine species and are caused by most types of ships. Since 2005, vessel strikes have been identified as a priority by the International Whaling Commission Conservation Committee (IWC-CC). The IWC-CC aims to identify at-risk populations and high-risk areas to develop and implement solutions to achieve a permanent reduction in vessel strikes. At least 75 marine species, including marine mammals, sea birds, and fish, are currently affected by vessel strikes (Schoeman et al. 2020). A vessel strike can cause several injuries, including propeller marks, bruises, fractures, hemorrhaging, and severed flukes, which can

---

[*]Corresponding author: lbaille@whoi.edu

Publisher: Inter-Research · www.int-res.com

lead to minor, severe, or fatal consequences to the animal (Jensen 2004).

Worldwide records show that many different types of ships are involved in whale strikes. Out of 134 recorded collisions between 1975 and 2002, Navy vessels, container/cargo ships/freighters, whale-watching ships, cruise ships/liners, and ferries were each responsible for 12–17% of the strikes (Jensen 2004). Recreational ships and steamships, Coast Guard ships, and fishing vessels each accounted for 3–7% of the collisions (Jensen 2004). Winkler et al. (2020) provided updated numbers on worldwide ship strikes involving cetaceans based on the IWC Ship Strike Database. Specifically, out of 402 cases (between 1820 and 2019), ferries, sailing yachts, cruise ships, and motor yachts were each responsible for 10–12.9% of the recorded strikes. Whale-watching vessels, Navy vessels, and container ships, and general cargo vessels each accounted for 6.2–8.4% of the collisions (Winkler et al. 2020).

### 1.1. North Atlantic right whales and vessel strikes

The North Atlantic right whale (NARW) *Eubalaena glacialis* is one of the world's most endangered large whale species, with approximately 360 individuals remaining in 2019 (Moore et al. 2021). Due to the low population size, high mortality rates, and low calving rates, this species has been classified as 'endangered' under the US Endangered Species Act since 1970 and is on the IUCN's 2020 Red List under the 'Critically Endangered' status (Cooke 2020). The range of the NARW spans from Florida (USA) to Iceland, while most of the animals are distributed along the eastern coasts of the USA and Canada (Gulf of Maine, Bay of Fundy, Gulf of St. Lawrence, Florida and Georgia seaboards) (Hunt et al. 2015). During the summer, NARWs aggregate in the north, specifically in the Bay of Fundy, on the Scotian Shelf, and in the Gulf of St. Lawrence, to feed on dense patches of copepods. In late fall, pregnant females and juveniles migrate to the southeastern coast of the USA, where females calve in mid-winter. Most males and non-pregnant females migrate to poorly documented wintering grounds (e.g. Nantucket Shoals, Georges Bank). In the spring, Cape Cod and the Great South Channel east of Cape Cod become the main migration destinations (Hunt et al. 2015). NARW habitat (calving and feeding grounds, migration routes) overlaps areas that are heavily affected by fishing activity, shipping traffic, and coastal runoff. This co-occurrence has earned this species the name of 'urban whale', and puts it especially at risk (Kraus & Rolland 2007).

NARWs have been observed to adapt their feeding strategy to follow the vertical distribution of copepods (Baumgartner & Mate 2003, Parks et al. 2012). Using time–depth recorders (TDRs), Baumgartner & Mate (2003) observed several whales performing deep-water summertime flat-bottom dives which were characterized by a rapid descent from the surface to the average depth of copepod density peaks (80–175 m). The whale stayed at such depths for 4 to 15 min before rapidly ascending back to the surface (Baumgartner & Mate 2003). On the other hand, using TDRs, Parks et al. (2012) witnessed surface feeding behaviors as whales actively fed at or just below the surface, where zooplankton concentrations peaked (Parks et al. 2012).

Fishing gear entanglement and vessel strikes are estimated to be responsible for the mortality and serious injuries of an average of 5.36 right whales per year (Hayes et al. 2018), which matches the 86 mortalities and serious injuries to NARWs recorded in the USA and Canada between 2000 and 2017 (NOAA Fisheries OPR 2020). While most large whale species are vulnerable to vessel strikes (Laist et al. 2001), NARWs are 2 orders of magnitude more prone to vessel strikes due to habitat exposure to several types of vessel (e.g. fast ferries, fishing vessels, cruise liners, naval ships, large container vessels) (Vanderlaan & Taggart 2007). While the actual number of mortalities caused by vessel strikes is difficult to assess (e.g. due to carcasses sinking or decomposing) (Laist et al. 2001, Henry et al. 2021), vessel collisions accounted for 52.5% of all deaths among necropsied right whales between 1970 and 2006 (Campbell-Malone et al. 2008). To address these threats, agencies such as the International Maritime Organization and National Oceanic and Atmospheric Administration established preventive measures, including implementing a series of regulations addressing collisions with vessels at sea.

### 1.2. Vessel strike mitigation strategies

A variety of mitigation measures have been developed to reduce the probability of vessel strikes with NARWs, starting in 2003 with the Bay of Fundy Traffic Separation Scheme (TSS) amendment (Vanderlaan et al. 2008). Vessel strike mitigation approaches can be classified into either large- or small-scale approaches. Large-scale approaches identify high-risk areas (e.g. Areas To Be Avoided [ATBAs], Dynamic Management Areas, Seasonal Management Areas, TSSs) and aim to increase NARW–boat separation by implementing a set of navigation rules, such as re-routing or speed reduction. Those measures may be permanent, seasonal, mandatory, or recommended, and may apply to all vessels or only a subset (Schoeman et al. 2020) (for details, see Text S1 in the Supplement at www.int-res.com/articles/suppl/n049p057_supp.pdf). Such mitigation strategies, when complied with, have led to a significant decrease in lethal strikes. Laist et al. (2011) and Conn & Silber (2013) observed half as many fatal injuries when ships were traveling under 10 knots (5.14 m $s^{-1}$) compared to higher speed ships. Vanderlaan & Taggart (2009) observed an 82% decrease in lethal strikes with NARWs upon implementing the Roseway Basin ATBA, Canada (Vanderlaan & Taggart 2009). On the other hand, small-scale approaches rely on individual vessels to detect at-risk animals and subsequently alter their course and speed to avoid collision (Text S2). Small-scale whale detections can be used to inform large-scale mitigation efforts about the presence of an animal at a given location and time.

In order to establish high-risk areas and/or to implement small-scale mitigation measures, a multitude of methods have been developed to detect large marine mammals, such as passive and active acoustic monitoring, marine mammal observers (MMOs), radio detection and ranging (RADAR), and thermal infrared imaging (thermal IR) (see Text S3). In this study, we evaluated the surface-based effectiveness of thermal IR systems as a surface detection method. This now cost-effective technology relies on the apparent temperature difference between the above-surface body parts of the animal or its exhalation and the ocean. This technology performs better in poor weather conditions compared to MMOs, can be used by day or at night, both on land (Zitterbart et al. 2020) and on vessels (Zitterbart et al. 2013), and has shown to reliably detect large whales up to several kilometers away (Zitterbart et al. 2020).

### 1.3. Agent-based simulation (ABS)

Agent-based simulation (ABS) is a simulation technique that consists of a system of autonomous entities, called agents. The relationships, interactions, and decisions among the agents, without the intervention of a centralized control, dictates the dynamics of the system (Chion 2011). Such simulations can provide valuable information on the dynamics of the real-world systems that they imitate (Bonabeau 2002). This concept became particularly popular in the field of ecology in the late 1980s following the growing accessibility of powerful computers (Huston et al. 1988). In the context of human–wildlife interactions, ABS is currently being used on a portion of the St. Lawrence River Estuary, Canada, as a decision support tool for boat–whale encounters and the sustainable management of human activities in this highly trafficked whale habitat (Chion 2011). This model simulated the spatiotemporal movement of marine mammals and boat traffic and allows testing of different zoning scenarios for boat traffic (e.g. seasonal closures, speed limits, re-routing), and boat traffic effects on marine mammals (Chion 2011).

The aim of our study was to assess the effectiveness of surface detection methods (i.e. detecting the animal when it is at the surface) for vessel strike mitigation using an ABS approach. The efficacy of surface-based detection systems is directly linked to vessel-specific characteristics, such as speed and maneuverability. We suggest that combining large- and small-scale mitigation strategies could lead to the highest level of protection for NARWs.

## 2. MATERIALS AND METHODS

### 2.1. WHorld (a simulated whale world environment)

In this study, a 3-dimensional grid was generated and virtual vessels and whales ('animats') were distributed randomly on that grid and instructed to move for 60 min (in model time). Each vessel was placed on the grid with a fixed speed and trajectory. Similarly, each animat was placed on the grid and instructed to move in the horizontal plane according to a correlated random walk, commonly used in mathematical modeling of animal movement (Codling et al. 2008), with a random ±5° change in heading between steps. The ±5° heading was chosen ad hoc in order to add some variability to the horizontal movement of the animat. This parameter is of negligible impact due the ship speed being much faster than the slow-swimming NARWs. Each animat was given a reasonable fixed speed (1, 2, or 3 m $s^{-1}$ [= 1.94, 3.88, or 5.82 knots]), and a uniquely generated dive profile (Hain et al. 2013). Table S1 summarizes the sets of parameters used for each of the simulated cases.

### 2.2. Vessels

We chose vessel system parameters to be broad enough so that they apply to a wide range of vessel

Table 1. Vessel parameters used for agent-based simulation

| Fixed parameter | Value | Unit |
|---|---|---|
| Vessel speed | 1–15 (1.94–29.15) | m s$^{-1}$ (knots) |
| Field of view | 20 | Degree |
| Reliable detection range | 500, 1000, 1500, 2000, 3000 | m |
| Reaction time | 60, 300, 600 | s |

categories. A summary of the vessel parameters used is provided in Table 1. We modeled vessel speeds from 1 to 15 m s$^{-1}$ (1.94–29.15 knots) to account for a wide range of vessels, from fishing boats to high-speed ferries. The field of view of the detection system was chosen to be 20°, which matches currently available systems. Furthermore, due to the speed difference between a transiting vessel and a NARW, with vessels usually traveling at higher speeds, it is very unlikely that a whale would enter the path of a vessel from beyond that field of view.

Each vessel was modeled with a specific and constant reliable detection range (RDR). The RDR is defined as the maximum distance at which a whale blow would be detected with certainty (probability of detection [PD] = 1). The RDR is dependent on weather conditions as well as the thermal IR system set up, particularly its elevation above the mean water level (Zitterbart et al. 2020). To account for a wide variety of vessel types, we defined the reaction time (RT) of a ship as the length of time a vessel requires to make an effective mitigation maneuver. This variable integrates covariates such as the maneuverability of the vessel, its ability to slow down, and the time needed between detection and action. RTs of 1 min apply to fully autonomous vessels with short lag times and to highly maneuverable ships, such as ferries, with dedicated observers to validate detections. RTs of 5 min apply to highly maneuverable vessels (ferries) that have longer alert and action times due to their lack of dedicated observers on-board. Finally, RTs of 10 min apply to poorly maneuverable vessels such as high-speed ferries and small container ships.

In our study, we assumed that a whale is in danger of a strike when it is within a certain range of the ship. We did not account for the severity of the strike.

### 2.3. Whales

Each animat followed an artificially generated dive profile. To mimic true NARW dive behavior, we extracted the diving characteristics from biologging data collected in the summers of 2000 and 2001 via suction-cup mounted TDRs (Baumgartner & Mate 2003, Baumgartner et al. 2017). Baumgartner & Mate (2003) focused on understanding the summertime foraging behavior of NARWs, which takes place in the type of habitat where the vast majority of NARW carcasses are typically found (Johnson et al. 2022, NOAA 2022). Hence, 90 % of our TDR data are composed of whales engaging in feeding behavior (Baumgartner & Mate 2003). Time–depth data from TDRs were manually selected and trimmed for quality control, e.g. removing time sections when the tag fell off the animal. Dive profiles were classified by a human analyst as either shallow or deep dives, depending on the behavior of the whale inferred from the dive profile. Subsequently, time–depth data were segmented into 3 depth layers: surface (0–5 m), subsurface (5–10 m), and deep (10+ m), as those sections determine the availability bias of the whale as well as its risk of vessel strikes. Those depth layers were associated with the respective behavioral states 1, 2, and 3 for modeling purposes. We used the distributions of frequency, duration, and number of transitions between depth sections to generate an artificial dive profile for each animat (Fig. 1). We added a state 0, which corresponds to the whale blowing at the water surface, making it available for detection. In both states 1 (0–5 m) and 2 (5–10 m), the whale is considered vulnerable to vessel strikes, as the hulls of many vessels can reach such depths, making vessel strikes with the diving animal possible. When a whale dives deeper than 10 m (state 3), it is considered out of reach of most non-container vessel hulls and therefore not susceptible to vessel strikes. Ultra-large container vessels that can have drafts up to 15.9 m were not considered in this study because we assume their maneuverability is so limited that effective mitigation measures in the form of evasive maneuvers could not be implemented with the currently available on-board surface-based detection technology (Zhang et al. 2021).

During the simulation, we studied 3 different animat behaviors for shallow, deep, and mixed diving behavior. Shallow and deep artificial dive profiles were exclusively generated from dive profiles classified as shallow and deep, respectively, while in mixed behavior, all dive profiles were considered. Except for one case (see Fig. 7C), where detection probabilities were computed for all 3 dive behaviors, and for the comprehensive plot summarizing in-time detection probability (ITDP; see Section 2.4) results for all possible parameter combinations (Fig. S1), the remainder of this study uses only the mixed diving behavior to better generalize.

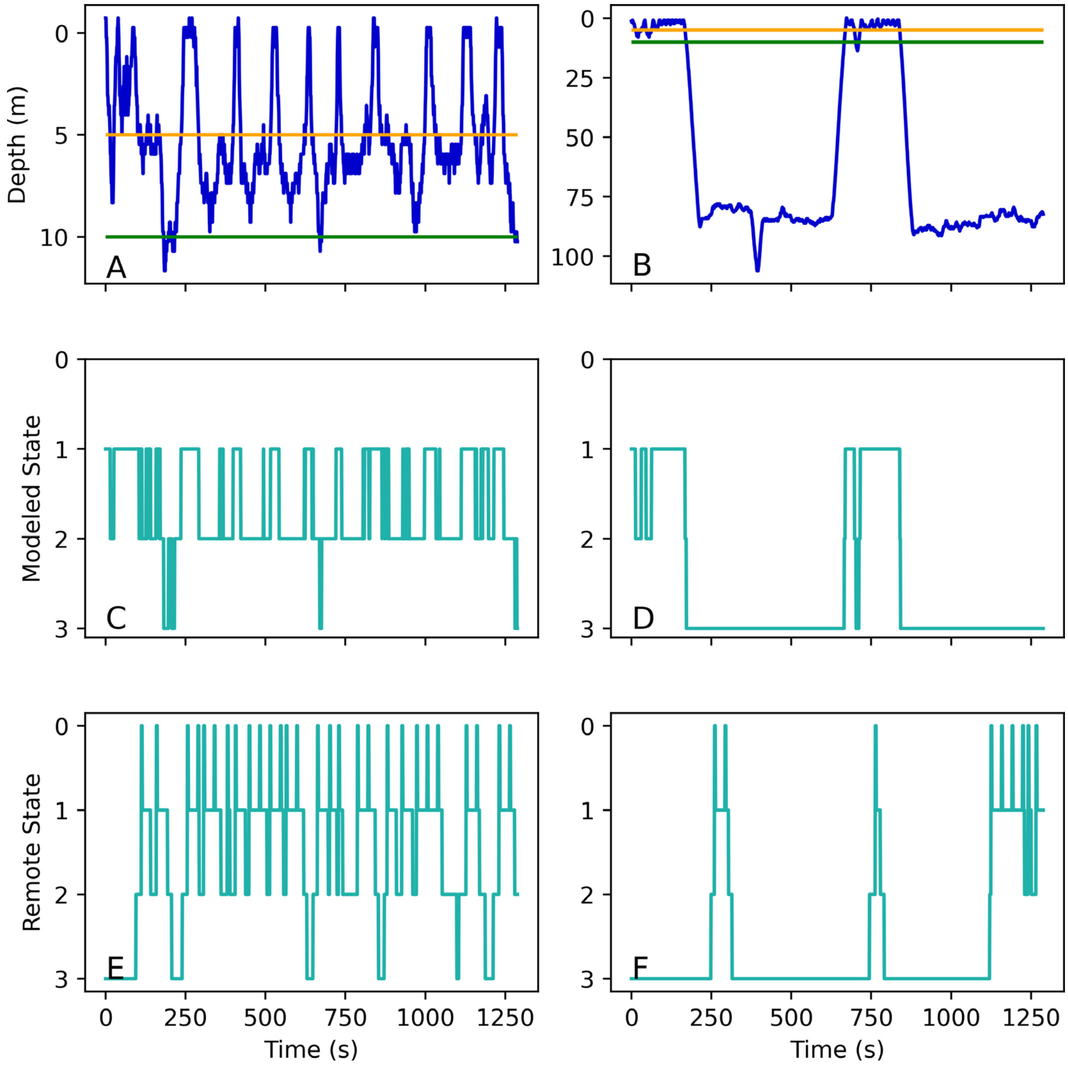

Fig. 1. Artificial dive profiles generated using a 3-step process, applied to (A,C,E) shallow dive behavior and (B,D,F) deep dive behavior. (A,B) True time-depth data collected via time−depth recorders. The horizontal 5 m (orange) and 10 m (green) lines mark the boundaries between states 1, 2, and 3 (where state 1 = depths of 0–5 m, state 2 = 5–10 m, state 3 = 10+ m). (C,D) Conversion from depth values to state values (0, 1, 2, 3) based on the respective true dive profiles from panels A and B. (E,F) Possible examples of modeled state dive profiles derived from the respective distributions of duration, occurrences, and number of transitions between depth sections of the true time−depth data. State 0 refers to whale exhalations that were artificially added at set intervals (inter-blow intervals) since collected time-depth data did not provide such information

In practice, exhalations of marine mammals are the main cue used by thermal imaging systems to detect large mammals (Zitterbart et al. 2013); therefore, in this study, an animat could only be detected when it was exhaling at the surface. From previous experiments, we estimated that an exhalation at the surface lasts about 3 s, and therefore set the duration of the blowing state (i.e. state 0) for this length of time in each dive profile (Zitterbart et al. 2013, 2020). When a whale was at the surface (state 1) for a prolonged amount of time (30+ s), we assumed that it would be taking breaths (i.e. blowing) at a regular interval, defined as the inter-blow interval (IBI). State transitions followed the logic described in Fig. 2, and an example of a segment of a dive profile is provided for additional clarity in Fig. 3.

### 2.4. Detection

We used a detection function, defined as the probability to detect a whale blow at a given distance, obtained during a previous experiment (Zitterbart et al. 2020). Humpback whale *Megaptera novaeangliae*

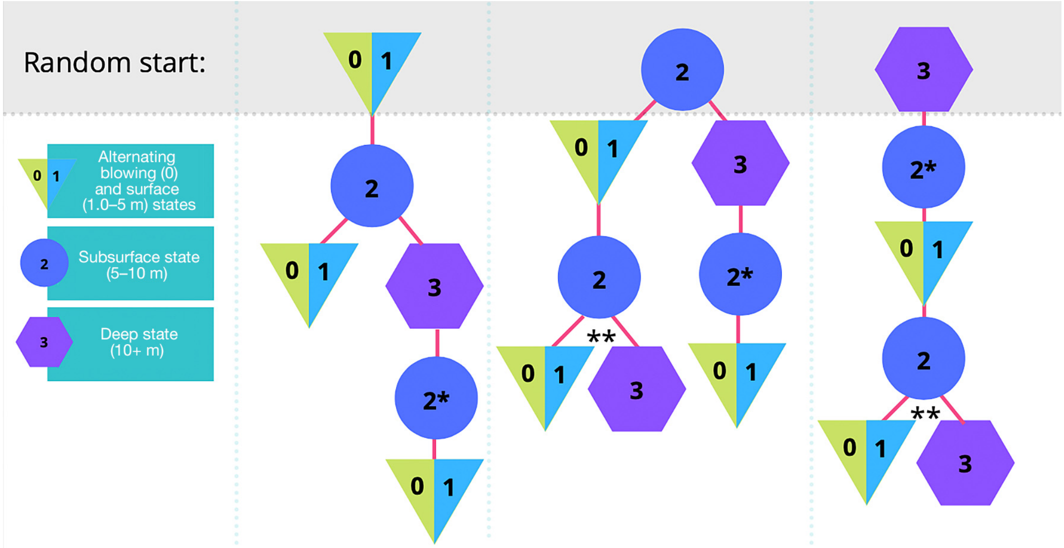

Fig. 2. State transitions depending on the random start of the dive profile. *After a deep dive (state 3), the animal must always return to the surface (state 1). **The animal can move from a subsurface state (2) to either a deep state (3) or the surface (1). The probability of a state change is chosen according to the transitions observed in the bio-logging data

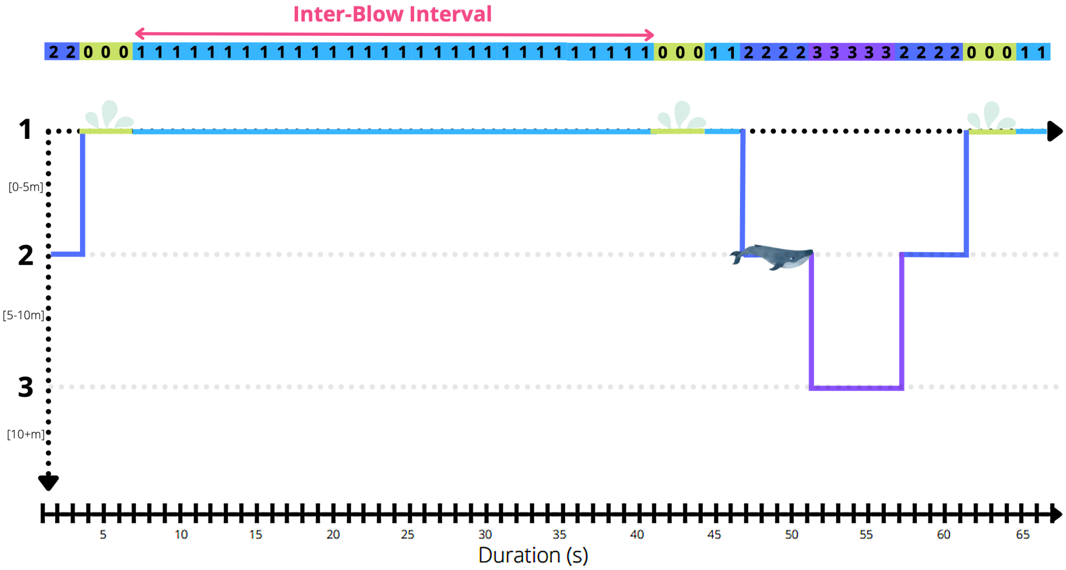

Fig. 3. Example of a segment of a dive profile, starting in state 2 (whale at 5–10 m depth) and a 30 s inter-blow interval (IBI). When the whale surfaces (transition of state 2 to state 1), it immediately breathes (state 1 to state 0) for 3 s. During its surface period (state 1), several breathing series (state 0) occur according to the IBI duration (30 s in this example). Note that this is a simplified and shortened dive profile example. Typical dive profiles have much longer segments for each state, with the exception of the artificially added blowing state (0) which always remains 3 s long

blow detection data were collected using a thermal IR imaging camera off Poipu Shores, Kauai (Hawaii, USA), in 2016, comparable to a point-transect distance sampling detection scheme. We derived the detection function by fitting a log-normal distribution to the detection data. The range at which the fitted detection function peaks (1600 m) was used as the furthest distance a whale blow would be detected with certainty (PD = 1), previously defined as the RDR. The detection function accounts for wind variability, as the whale blow detections used to create the function were collected in wind forces ranging from 1 to 4 BFT (Beaufort scale) (Zitterbart et al. 2020). Impacts of the visibility on the detection function are explicitly accounted for by varying the location of the RDR.

We made the assumption that there is a relationship between the body volume or mass of the animal and its blow size. Since NARWs (70 t; Burnie & Wil-

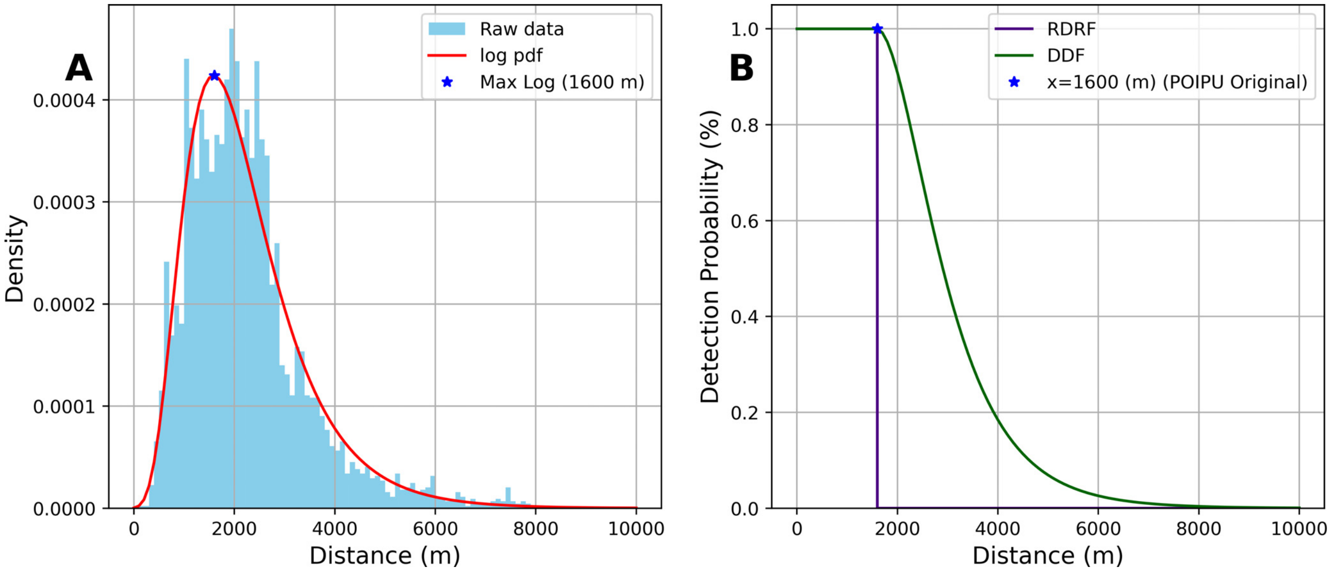

Fig. 4. (A) Density distribution of detected blows, from humpback whales, as a function of distance. The data were collected in 2016 off the Poipu Shores, Hawaii (USA), using a thermal infrared imaging camera located 16 m from the mean water level. A log-normal function (log probability density function [pdf], red) was fitted to the raw distribution. The maximum value reached by the log pdf is marked with a blue star (max log) at 1600 m and depicts the reliable detection range (RDR). (B) RDR function (RDRF, purple) vs. data-driven detection function (DDF, green) scenarios. For detection distances ≤RDR, the probability of detection equals 1 in both scenarios. However, past the RDR value, in the RDRF scenario, the probability of detection drops to 0, while in the DDF scenario, it logarithmically decreases to 0

son 2001) are much larger than humpback whales (30 t; Cabanillas & Ayma 2021), we expected the exhalations of NARWs to be at least of the same volume or larger than those of humpback whales. Therefore, we expected that using a humpback whale detection function to simulate NARWs was a rather conservative approach.

To assess the impact of the shape of the detection function, i.e. detections beyond RDR (PD < 1), we tested 2 different scenarios. In the RDR function (RDRF) scenario, the detection probability is binary, set to 1 for ranges below or equal to RDR, and 0 for ranges beyond RDR. In the data-driven detection function (DDF) scenario, the detection probability is set to 1 for ranges below or equal to RDR, and then logarithmically decreases for ranges beyond RDR as depicted in Fig. 4. To test different RDRs, either in the RDRF or DDF scenarios, the detection function was simply moved along the *x*-axis, while the shape of the detection function was kept similar as illustrated in Fig. S2.

In every operational setting, DDF is the realistic detection case, and the RDRF scenario is only relevant for academic purposes. Hence, with the exception of one case (see Fig. 6A), which compares detection probability results when using RDRF vs. when using DDF, the remainder of this article will only consider the DDF case, as the latter leads to realistic detection results.

For successful mitigation, a whale needs to be detected early enough (in-time) so the vessel can still take evasive actions (Zitterbart et al. 2013). This can be parameterized with the definition of a safe zone and a danger zone (Fig. 5). We defined the danger zone as the area where, if a whale were detected there, the vessels would be too close to safely maneuver to avoid a strike. The danger zone range (DZR) is derived from the vessel speed and the RT (DZR = RT × vessel speed). On the other hand, the safe zone represents the area from the DZR to the maximum detection range. When a whale is detected in the safe zone, a vessel has enough time to implement the necessary measures to safely alter its trajectory and avoid a strike. In this study, detection occurs 'in-time' when a whale is detected in the safe zone prior to entering the danger zone.

We define the ITDP as our metric to evaluate the impact of the different vessel and whale parameters. All whales were initially placed outside the danger zone, and only whales that would enter that zone were considered. The ITDP is defined as the proportion of whales that were detected in the safe zone from all whales that entered the danger zone. The simulation code and supporting data can be found at https://github.com/whoi-mars/WHorld_public.git.

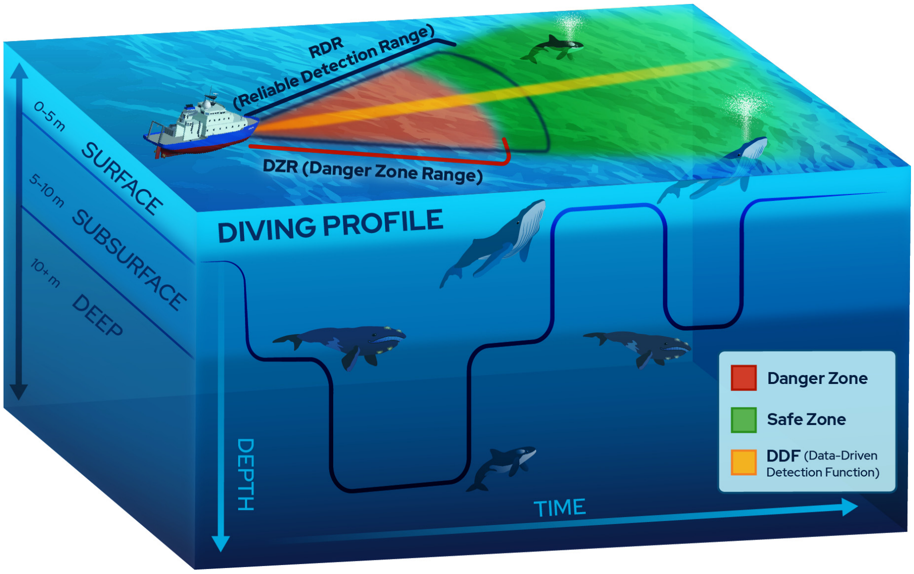

Fig. 5. Definitions of relevant areas and dive states. The detection area of a surface-based detection system with a 20° field of view is divided into a danger zone and a safe zone, which depend on vessel speed, vessel reaction time, and the reliable detection range (RDR) of the mitigation system. For the purpose of this study, the whales' possible depths were divided into 3 categories: surface (0–5 m), subsurface (5–10 m), and deep (10+ m). Only whales that are at the surface and blowing can be detected by a vessel

## 3. RESULTS

### 3.1. Detection function shape

We found that the shape of the detection function (Fig. 4B; Fig. S2) has a significant impact on the ITDP. When we did not consider whales that are located beyond the RDR (RDRF scenario, 1000 m; Fig. 6A), the ITDP drops to values below 90% for vessel RTs above 1.5 min, and to 0 for RTs above 3 min (Fig. 6A). This can be explained by the linear increase of the danger zone with RT, for a given speed (5 m s$^{-1}$ or 9.7 knots in this example). Due to a fixed detection range, a larger danger zone reduces the safe zone and vice versa. Beyond a certain RT, the DZR will be larger than the RDR, and thus the ITDP will be zero. In contrast, if detections beyond RDR are considered (DDF case), the ITDP does not drop below 90% even when RT = 10 min, which we consider to be a very long RT. This is explained by the fact that animals can be detected further out, hence are available for detection in the safe zone more frequently.

### 3.2. Vessel-based factors

The RDR is one of the main factors that determines the size of the safe zone. At a given vessel speed and RT, the danger zone is constant in size, hence with increasing RDR, only the safe zone increases. As expected, with increasing RDR (i.e. increasing safe zone), ITDP values increase as well (Fig. 6B).

The impact of RT on the ITDP is highly dependent on vessel speed. For short RTs, the ITDP is not significantly impacted by increasing vessel speeds (at most a 2% decrease across vessel speeds [1–15 m s$^{-1}$, 1.9–29.2 knots] when RT = 1 min). On the other hand, longer RTs are very sensitive to higher vessel speeds, with a decrease of up to 90% when comparing the ITDP of RT = 10 min at vessel speeds of 5 m s$^{-1}$ (9.7 knots) vs. 15 m s$^{-1}$ (29.2 knots). At low vessel speeds ($\leq$5 m s$^{-1}$), the impact of RT is at most a 10% decrease (RT = 1 vs. 10 min), compared to 90% for high vessel speeds (10 m s$^{-1}$, 19.4 knots) (Fig. 6C). This can be explained by higher RTs leading to larger danger zones, which increase the probability of a detectable whale surfacing in that zone rather than in the safe zone. It is noteworthy that the ITDP decreases by up to 81% (47–81%) when comparing results obtained at vessel speeds of 5 vs. 10 m s$^{-1}$ (9.7 vs. 19.4 knots) for RT = 10 min.

### 3.3. Whale-based factors

We found that the swimming speed of the animal has no effect on the ITDP (Fig. 7A). This can be explained by the speed difference between the animal and the vessel. At slow vessel speeds, the safe zone is much larger than the danger zone, thus the animal is often available for detection regardless of its speed. At higher vessel speeds, the ITDP drops. The decrease of the ITDP is independent from the speed of the whale and is only caused by increasing

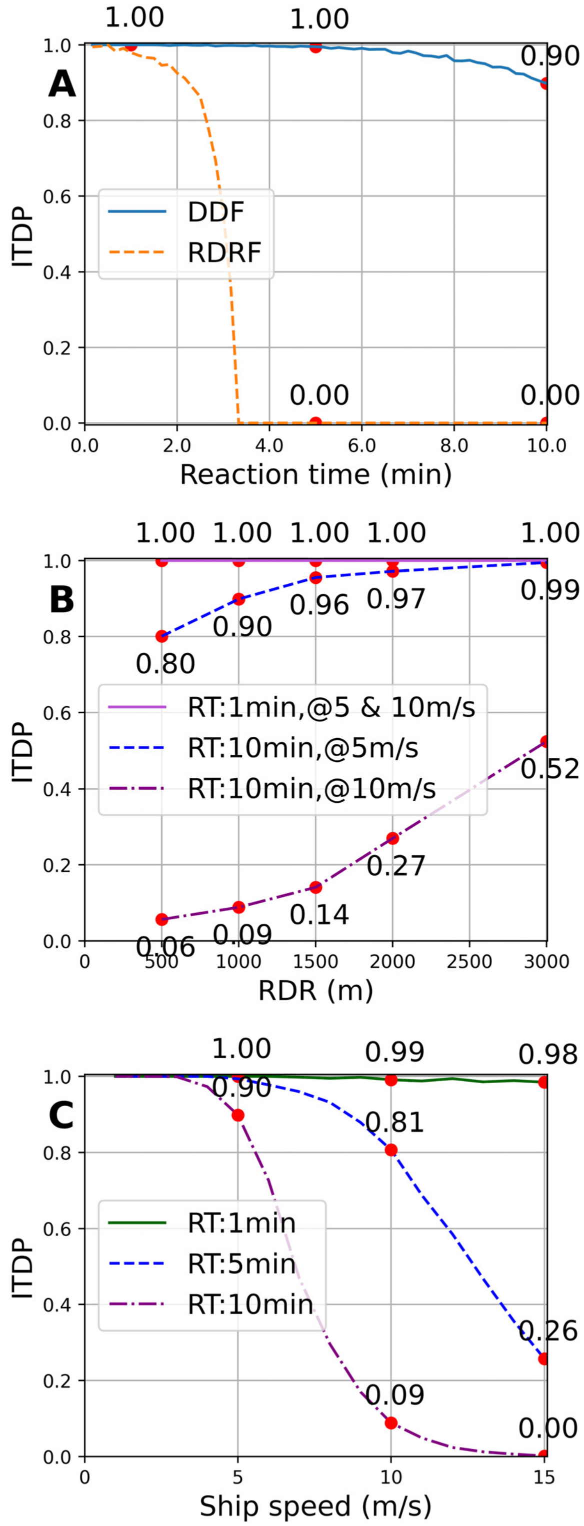

Fig. 6. In-time detection probability (ITDP) as a function of different vessel-based parameters. (A) Reaction time (RT) for the 2 detection scenarios (reliable detection range function [RDRF] vs. data-driven detection function [DDF]). (B) RDRs (500–3000 m) for varying RTs (1, 10 min) and vessel speeds (5, 10 m $s^{-1}$). (C) RTs (1, 5, 10 min) as a function of ship speeds. All scenarios used DDF, RDR = 1000 m, inter-blow interval = 60 s, a mixed diving behavior, and RT = 300 s unless indicated otherwise

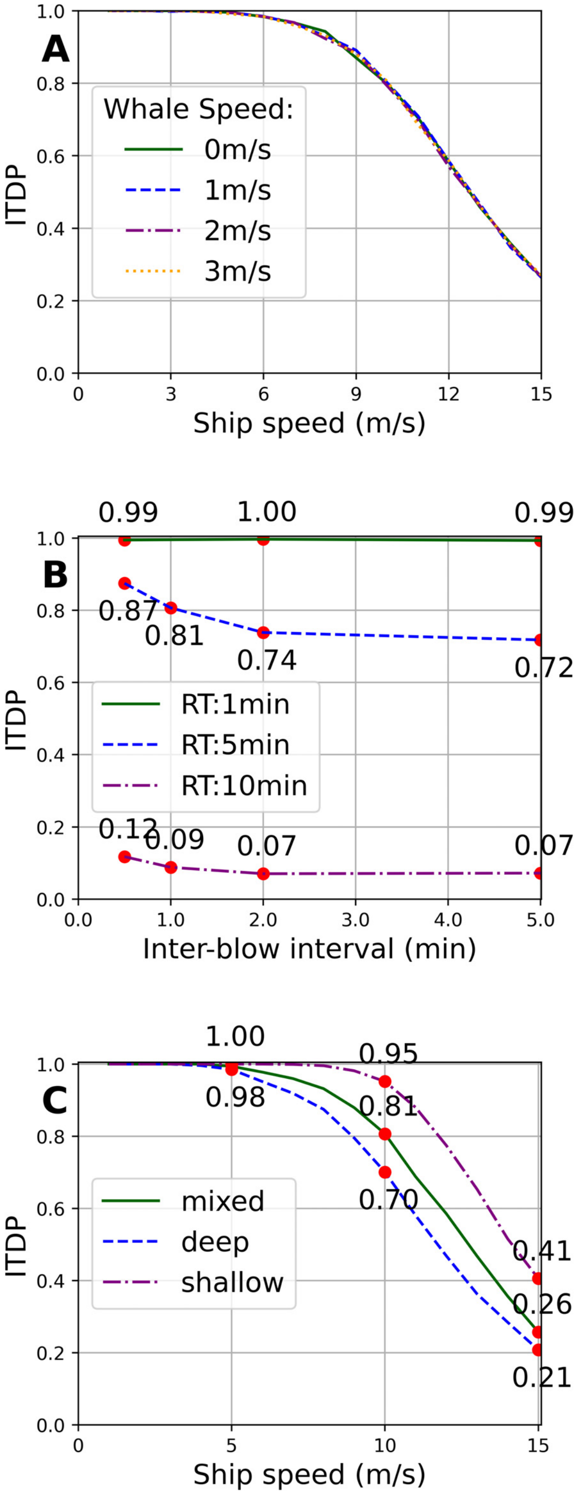

Fig. 7. In-time detection probability (ITDP) as a function of different whale-based parameters. (A) Whale speed (0, 1, 2, 3 m $s^{-1}$) as a function of ship speeds (0–15 m $s^{-1}$). (B) Inter-blow intervals (IBIs: 30, 60, 120, 300 s) for different reaction times (RTs: 1, 5, 10 min). (C) Whale dive profile behavior (mixed, shallow, deep) as a function of ship speeds. All scenarios used data-driven detection functions, reliable detection range = 1000 m, IBI = 60 s, a mixed diving behavior, and RT = 300 s unless indicated otherwise

vessel speeds which increase the DZR (DZR = RT × vessel speed). For the whale's speed to have an impact on the ITDP, the animal would need to be swimming at equal or higher speeds than the vessel and directly into the danger zone for a prolonged duration. This is an unrealistic scenario, as NARWs are slow swimmers (0.36 m $s^{-1}$ or 0.7 knots), with a maximum recorded swimming speed reaching only 1.5 m $s^{-1}$ or 2.9 knots (Hain et al. 2013). Even when simulating double the known maximum whale speed (3 m $s^{-1}$ or 5.8 knots), no impact on the ITDP can be observed. Fig. S3 comprehensively summarizes the ITDP results as a function of ship speeds for varying whale speeds.

Since IBI data were not readily available, we simulated a range of possible IBIs (30, 60, 120, and 300 s) where each blow is detectable for 3 s. We found that the IBI does not reduce the ITPD by more than 15% (vessel speed = 10 m $s^{-1}$ [19.4 knots], RDR = 1000 m). In this case, we chose a rather high vessel speed of 10 m $s^{-1}$ compared to the other results presented, which were evaluated at 5 m $s^{-1}$ (9.7 knots) vessel speed, because at 5 m $s^{-1}$, the impact of the IBI is negligible. Furthermore, the impact of IBI on the ITDP is only visible for RTs larger than 300 s. For RT = 300 s (5 min), Fig. 7B shows a 15% decrease in ITDP between IBI = 30 s (ITDP = 0.87%) and IBI = 5 min (ITDP = 0.72%). Similarly, for RT = 10 min, the ITDP almost halves between IBI = 30 s (ITDP = 0.12%) and IBI = 5 min (ITDP = 0.7%). Overall, the impact of the IBI can be considered rather small.

Diving behavior of NARWs changes significantly throughout the year, depending on either the food availability at different depths of the ocean or the behavioral state of the animal (breeding vs. foraging) (Murison & Gaskin 1989). At low vessel speeds (≤5 m $s^{-1}$ or ≤9.7 knots), the behavior of the whale has negligible impact on the ITDP (98–100%) (Fig. 7C). The diving behavior of the whale starts to have an impact at higher vessel speeds. At 10 m $s^{-1}$ (19.4 knots), there is a 25% decrease in ITDP between shallow and deep dives. This observation can be explained by the fact that if the whale is on a deep dive, it is less often available for detection, i.e. fewer surfacing events reduce the chances of detection in the safe zone, making the animal more vulnerable to strikes.

## 4. DISCUSSION

Current mitigation measures have not been effective enough to entirely prevent vessel strikes of NARWs and other large whale species (Davies & Brillant 2019). Re-routing measures and speed-restricted zones have been shown to effectively decrease the rate of strikes, as well as the severity of injury (Vanderlaan & Taggart 2009). However, those measures rely on the compliance of mariners, which can be low (McKenna et al. 2012, Silber et al. 2012). Hence, increased enforcement, when resources and geography allow, might be necessary to improve the effectiveness of those measures (Schoeman et al. 2020). Additionally, re-routing measures might help protect one species, but put another one at higher risk (Redfern et al. 2013). The purpose of our model was to assess in which scenarios, i.e. for which vessel and whale parameter combinations, an on-board IR vessel strike mitigation system would enhance the protection of large whales. While this study focuses only on thermal imaging systems, our model is applicable to any surface-based detection method as long as the detection function is known.

### 4.1. Vessel parameter dependency

Here, we found that in slow-speed environments, such as speed-restricted zones, vessel-based whale detection systems for strike mitigation could provide a high level of protection for the animals. Specifically, if a vessel travels slowly (5 m $s^{-1}$, 9.7 knots), any form of detection system with at least 1000 m of RDR will lead to high ITDPs (>90%). Detection ranges of 1000 m can be achieved on the majority of vessels that provide >5 m elevation (Zitterbart et al. 2020). Due to the slow vessel speed, parameters such as the RT of the vessel become less relevant. The RT of a vessel is mainly determined by its maneuverability (which cannot be changed) and the time between detection and action. The fact that the RT is less relevant during slower travel is a key finding, as it opens up the possibility for remote validation of vessel-based detections reducing the active involvement of the vessel crew. One could imagine a system where automatic detections are transmitted to a data center in near-real time and validated immediately. Turnaround times would likely be on the order of minutes, short enough to alert the vessel about the whale's presence without any false alerts. We consider false alerts to be a major reason why automatic vessel-based whale detection systems could not be directly used by the vessel crew. Frequent alarms lead to alarm fatigue (Blum & Tremper 2010); hence, we speculate that even at relatively low false alert rates (6 $h^{-1}$, Zitterbart et al. 2013), crews are likely to soon ignore warnings.

In areas where vessel speed is not regulated and vessels travel at higher speeds (5–15 m $s^{-1}$, 9.7–29.2 knots), we group vessels into 3 classes. When vessels have a high maneuverability and the ability to change velocity quickly (e.g. certain fishing vessels and ferries), vessel-based whale detection systems would be very effective (ITDP > 98%), under the conditions that the RDR is at least 1 km and that the time from detection to action is minimal (on the order of seconds). Currently, such conditions could only be met with dedicated observers on-board, who could either be scanning the ocean surface, or validating automatic detections provided by a whale detection system. Obtaining such a quick response comes with great efforts and costs (Verfuss et al. 2018), and hence is unlikely to be implemented on a large scale. For vessels with longer RTs (lower maneuverability and/or longer detection-to-action time), a whale detection system can still be effective if the RDR is increased to several kilometers (+58% ITDP at RDR = 3000 m vs. RDR = 1000 m when RT = 5 min and vessel speed = 15 m $s^{-1}$ or 19.2 knots). This is valid for a large group of vessels (e.g. cruise vessels) that have high enough elevations to provide far detection ranges for the whale detection system (Zitterbart et al. 2020). Thus, longer RTs can be offset by more advanced detection systems with larger RDRs or by reducing vessel speed. However, for vessels that travel at very high speeds, have very poor maneuverability, and might travel in shipping lanes, where quick maneuvers are not feasible (e.g. supertankers, large container vessels), no currently available vessel-based detection methods would provide enough detection range for effective protection. In order for them to benefit from surface-based detection methods, the detection range of the system (RDR) needs to be significantly increased. This can be done by increasing the elevation of the detection system with respect to the mean water level. We have previously achieved RDR larger than 6 km by placing thermal IR systems on elevated locations on land. For vessels, one could envision a detection system that is either held up high behind the ship (i.e. via a kite) or flying ahead of the vessel (i.e. drone).

### 4.2. Whale parameter dependency

Another finding of this simulation study is that animal behavioral factors such as swimming speeds, diving profiles, and the IBI are not as impactful on the ITDP as the vessel parameters. Our simulation showed that varying whale speeds does not have any impact on the ITDP. In the case of NARWs, the animals' horizontal movements do not need to be considered for the design of vessel-based detection systems (e.g. field of view), which can have a significant impact on the system costs, and potentially negatively impact their wide-spread use.

Our study shows that NARWs on deep foraging dives have a lower ITDP compared to surface-feeding NARWs (25% decrease at 10 m $s^{-1}$ [19.4 knots] vessel speed) because they surface less often and hence are available for detection less often. However, our study also highlights that NARW behavior is only relevant when vessels are traveling at high speeds (10+ m $s^{-1}$, 19.4+ knots). Slower vessels have an equally high ITDP (98+%) regardless of the NARW diving behavior (Fig. 7C). Hence, a large-scale mitigation measure, such as a speed restriction zone, would help alleviate the impact of diving behavior and make the use of vessel-based mitigation systems most effective.

### 4.3. Limitations and future work

In this study, the impact of the weather and vessel strike location were not studied explicitly. The impact of weather conditions on the detection function has been previously studied (Zitterbart et al. 2020) and implicitly included in our model through the RDR. In follow-up studies, the model could be extended by making it adaptable to specific regions of the ocean to account for specific local atmospheric (clear, rainy, foggy) and oceanic (wave height) conditions, and associated RDRs. Additionally, the bio-logging data used to create unlimited dive profiles were collected in foraging areas. Therefore, this study lacks dive profile observations in breeding or calving grounds. Our findings reveal little impact of animal behavior on the ITDP, but if specific efficacy estimates are required for breeding grounds and during migration, dive profiles collected during such behaviors are needed. Finally, while this study focuses on NARWs, this same model could easily be adapted to other marine species by adjusting the animal parameters (dive profiles, swimming speeds, species-dependent detection functions).

## 5. CONCLUSIONS

This study revealed that the probability of detecting a whale early enough to still take evasive actions predominantly depends on the vessel parameters (vessel speed and maneuverability) and the performance of the detection system employed, rather than on the behavior of the whales. We also conclude that surface-based whale detection may be very effective for whale-strike mitigation, and a large-scale deployment on suitable vessels of such systems in high-risk areas could effectively reduce whale strikes, especially when combined with large-scale mitigation measures, such as speed restrictions.

While certain vessel classes cannot directly benefit from currently available vessel-based whale detection systems, the information obtained and shared from other vessels equipped with such systems could help estimate a near real-time distribution of whales in critical areas and improve the large-scale dynamic management efforts. With future technological improvements on the hardware (larger detection ranges) and software (fewer false positives), vessel strike mitigation systems could become a standard tool in the maritime industry.

*Acknowledgements*. This work was supported by the US Navy Office of Naval Research (ONR) under award number N000141912669. We thank Mark Baumgartner for providing North Atlantic right whale dive profile data collected in 2000 and 2001. The preprint version of this paper can be found on bioRxiv (https://www.biorxiv.org/content/10.1101/2021.08.27.457997v1).

## LITERATURE CITED

Baumgartner MF, Mate BR (2003) Summertime foraging ecology of North Atlantic right whales. Mar Ecol Prog Ser 264:123–135

Baumgartner M, Wenzel FW, Lysiak NSJ, Patrician MR (2017) North Atlantic right whale foraging ecology and its role in human-caused mortality. Mar Ecol Prog Ser 581: 165–181

Blum JM, Tremper KK (2010) Alarms in the intensive care unit: Too much of a good thing is dangerous: Is it time to add some intelligence to alarms? Crit Care Med 38: 702–703

Bonabeau E (2002) Agent-based modeling: methods and techniques for simulating human systems. Proc Natl Acad Sci USA 99(Suppl 3):7280–7287

Burnie D, Wilson DE (2001) Animal: the definitive visual guide to the world's wildlife. Dorling Kindersley, New York, NY

Cabanillas AC, Ayma VH (2021) Humpback whale's flukes segmentation algorithms. In: In: Lossio-Ventura JA, Valverde-Rebaza JC, Díaz E, Alatrista-Salas H (eds) Information management and big data. SIMBig 2020, Lima, Oct 1–3 2020. Commun Comput Inform Sci 1410: 291–303

Campbell-Malone R, Barco SG, Daoust PY, Knowlton AR, McLellan WA, Rotstein DS, Moore MJ (2008) Gross and histologic evidence of sharp and blunt trauma in North Atlantic right whales (*Eubalaena glacialis*) killed by vessels. J Zoo Wildl Med 39:37–55

Chion C (2011) An agent-based model for the sustainable management of navigation activities in the Saint Lawrence Estuary. PhD thesis, Université du Québec, Montreal

Codling EA, Plank MJ, Benhamou S (2008) Random walk models in biology. J R Soc Interface 5:813–834

Conn P, Silber G (2013) Vessel speed restrictions reduce risk of collision-related mortality for North Atlantic right whales. Ecosphere 4:art43

Cooke JG (2020) *Eubalaena glacialis* (errata version published in 2020). The IUCN Red List of Threatened Species. e.T41712A178589687. https://dx.doi.org/10.2305/IUCN.UK.2020-2.RLTS.T41712A178589687.en

Davies KT, Brillant SW (2019) Mass human-caused mortality spurs federal action to protect endangered North Atlantic right whales in Canada. Mar Policy 104:157–162

Hain JHW, Hampp JD, McKenney SA, Albert JA, Kenney RD (2013) Swim speed, behavior, and movement of North Atlantic right whales (*Eubalaena glacialis*) in coastal waters of northeastern Florida, USA. PLOS ONE 8:e54340

Hayes SA, Josephson E, Maze-Foley K, Rosel PE (2018) US Atlantic and Gulf of Mexico Marine Mammal Stock Assessments – 2017, 2nd edn. Tech Rep NMFS-NE-245. US Department of Commerce, National Oceanic and Atmospheric Administration, National Marine Fisheries Service

Henry AG, Garron M, Morin D, Smith A, Reid A, Ledwell W, Cole TVN (2021) Serious injury and mortality determinations for baleen whale stocks along the Gulf of Mexico, United States East Coast, and Atlantic Canadian Provinces, 2014–2018. Northeast Fisheries Science Center Ref Doc 21-07. US Department of Commerce, National Oceanic and Atmospheric Administration, National Marine Fisheries Service

Hunt KE, Rolland RM, Kraus SD (2015) Conservation physiology of an uncatchable animal: the North Atlantic right whale (*Eubalaena glacialis*). Integr Comp Biol 55:577–586

Huston M, DeAngelis E, Post W (1988) New computer models unify ecological theory. Bioscience 38:682–691

Jensen AS (2004) Large whale ship strike database. NOAA Tech Memo NMFS-OPR; 25. US Department of Commerce, National Oceanic and Atmospheric Administration, Silver Spring, MD

Johnson CM, Reisinger RR, Palacios DM, Friedlaender AS and others (2022) Protecting blue corridors – challenges and solutions for migratory whales navigating international and national seas. Tech Rep. WWF. https://doi.org/10.5281/zenodo.6196131

Kraus SD, Rolland (eds) (2007) The urban whale: North Atlantic right whales at the crossroads. Harvard University Press, Cambridge, MA

Laist DW, Knowlton AR, Mead JG, Collet AS, Podesta M (2001) Collisions between ships and whales. Mar Mamm Sci 17:35–75

McKenna MF, Katz SL, Condit C, Walbridge S (2012) Response of commercial ships to a voluntary speed reduction measure: Are voluntary strategies adequate for mitigating ship-strike risk? Coast Manag 40:634–650

Moore MJ, Rowles TK, Fauquier DA, Baker JD and others (2021) Assessing North Atlantic right whale health: threats, and development of tools critical for conservation of the species. Dis Aquat Org 143:205–226

Murison LD, Gaskin DE (1989) The distribution of right whales and zooplankton in the Bay of Fundy, Canada. Can J Zool 67:1411–1420

NOAA (2022) 2017–2022 North Atlantic right whale unusual mortality event. https://www.fisheries.noaa.gov/national/marine-life-distress/2017-2022-north-atlantic-right-whale-unusual-mortality-event

NOAA Fisheries OPR (Office of Protected Resources) (2020) North Atlantic right whale (*Eubalaena glacialis*) vessel speed rule assessment. Tech Rep. https://media.fisheries.noaa.gov/2021-01/FINAL_NARW_Vessel_Speed_Rule_Report_Jun_2020.pdf

Parks SE, Warren JD, Stamieszkin K, Mayo CA, Wiley D (2012) Dangerous dining: Surface foraging of North Atlantic right whales increases risk of vessel collisions. Biol Lett 8:57–60

Peel D, Smith JN, Childerhouse S (2018) Vessel strike of whales in Australia: the challenges of analysis of historical incident data. Front Mar Sci 5:69

Redfern JV, McKenna MF, Moore TJ, Calambokidis J and others (2013) Assessing the risk of ships striking large whales in marine spatial planning. Conserv Biol 27: 292–302

Schoeman RP, Patterson-Abrolat C, Plön S (2020) A global review of vessel collisions with marine animals. Front Mar Sci 7:292

Sèbe M, Kontovas CA, Pendleton L (2019) A decision-making framework to reduce the risk of collisions between ships and whales. Mar Policy 109:103697

Silber GK, Adams JD, Bettridge S (2012) Vessel operator response to a voluntary measure for reducing collisions with whales. Endang Species Res 17:245–254

UNCTAD (United Nations Conference on Trade and Development) (2020) Review of maritime transport 2020. Tech Rep. https://unctad.org/system/files/official-document/rmt2020_en.pdf

Vanderlaan ASM, Taggart CT (2007) Vessel collisions with whales: the probability of lethal injury based on vessel speed. Mar Mamm Sci 23:144–156

Vanderlaan ASM, Taggart CT (2009) Efficacy of a voluntary area to be avoided to reduce risk of lethal vessel strikes to endangered whales. Conserv Biol 23:1467–1474

Vanderlaan ASM, Taggart CT, Serdynska AR, Kenney RD, Brown MW (2008) Reducing the risk of lethal encounters: vessels and right whales in the Bay of Fundy and on the Scotian Shelf. Endang Species Res 4:283–297

Verfuss UK, Gillespie D, Gordon J, Marques TA and others (2018) Comparing methods suitable for monitoring marine mammals in low visibility conditions during seismic surveys. Mar Pollut Bull 126:1–18

Winkler C, Panigada S, Murphy S, Ritter F (2020) Global numbers of ship strikes: an assessment of collisions between vessels and cetaceans using available data in the IWC ship strike database. IWC/68B/SC HIM09. International Whaling Commission, Cambridge

Zhang M, Yu H, Feng G, Ren H (2021) Investigation on effects of springing and whipping on fatigue damages of ultra-large container ships in irregular seas. J Mar Sci Technol 26:432–458

Zitterbart DP, Kindermann L, Burkhardt E, Boebel O (2013) Automatic round-the-clock detection of whales for mitigation from underwater noise impacts. PLOS ONE 8:e71217

Zitterbart DP, Smith HR, Flau M, Richter S and others (2020) Scaling the laws of thermal imaging-based whale detection. J Atmos Ocean Technol 37:807–824

*Editorial responsibility: Robin W. Baird,*
*Olympia, Washington, USA*
*Reviewed by: J. N. Smith and 1 anonymous referee*

*Submitted: September 1, 2021*
*Accepted: July 6, 2022*
*Proofs received from author(s): September 22, 2022*